Double Corrugated Waveguide for Ka-Band Traveling Wave Tube

Claudio Paoloni, *Senior Member, IEEE*, Mauro Mineo, Manju Henry, and Peter G. Huggard, *Senior Member, IEEE*

***Abstract*— The double corrugated waveguide (DCW), incorporating a row of metallic pillars on each side of the electron beam, is demonstrated as a promising slow-wave structure for millimeter wave, Ka-band, traveling wave tubes (TWTs). Different configurations, including novel bent couplers with tapered pillars, have been designed, realized, and validated by S-parameter measurements. The design and simulation of a DCW TWT demonstrated very good performance in the frequency band 32–37 GHz. The ease of fabrication and assembly make the DCW a suitable basis for a new generation of millimeter wave TWTs.**

***Index Terms*— Double corrugated waveguide (DCW), microfabrication, millimeter waves, satellite communications, slow-wave structures (SWSs), traveling wave tubes (TWTs).**

I. Introduction

MILLIMETER wave traveling wave tubes (TWTs) are key devices when wideband, medium power amplification, and compact dimensions are required. The development of power amplifiers with GaN transistors has been a breakthrough in the field of millimeter wave amplification. They present a credible replacement for vacuum electronic technology in a number of microwave applications. However, the TWTs continue to monopolize the communication satellite payloads due to their reliability, robustness against high thermal stress, and ionizing radiation typical of the space environment. Furthermore, the TWTs provide at least one order of magnitude higher output power than solid-state devices in millimeter wave frequency range [1]–[5]. A lifetime in term of tens of thousand hours is assured by the well-established cathode technology.

In contrast to the solid-state power amplifiers, which are realized by high volume semiconductor manufacturing processes, the TWT production requires the assembly of numerous tight tolerance parts. This results in relatively low yield and high fabrication costs, costs that increase as the operating frequency rises [6].

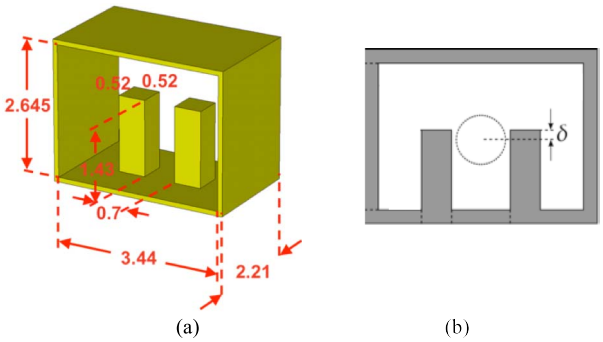

Fig. 1. (a) Schematic of a section of DCW containing two rows of square pillars. Dimensions (mm) have been optimized for wideband interaction, 32–37 GHz, with 12-kV electron energy. (b) cross section.

To give more details, the TWTs are typically based on a helical slow-wave structure (SWS). Such helix-based tubes can provide multioctave bandwidths and output powers above 100 W up to 50 GHz.

However, the helix has to be held concentrically by a number of longitudinal dielectric supports in a metallic cylindrical envelope. Each of those subcomponents must be precisely manufactured and assembled. Verification of the performance of a helix TWT is usually performed after the tube is sealed. Adjustments are possible mainly by varying the beam voltage. The decrease in diameter of the helix with increasing operating frequency, e.g., about 200 μm at 50 GHz, makes fabrication very demanding and impractical above about 65 GHz.

The high cost of millimeter wave TWTs currently limits their use in specific applications in space and defense fields. The availability of cost effective TWTs would be of great benefit for numerous millimeter wave applications, for example as wireless base stations for high-speed communications or for high-data rate satellite communications. A sensible cost reduction can be achieved only by the introduction of SWSs that are easier to fabricate and assemble [7], [8].

The all-metal double corrugated waveguide (DCW) was conceived to solve the formidable fabrication challenges posed by the need for an SWS for the 1-THz vacuum tube [9], [10]. The DCW consists of two parts: 1) a channel waveguide with two rows of pillars that define the beam channel and 2) a lid to close the structure (Fig. 1). The electron beam/electromagnetic

Manuscript received August 6, 2015; revised September 11, 2015; accepted September 16, 2015. Date of current version October 20, 2015. This work was supported by the Science and Technology Facilities Council under Grant ST/L003406/1. The review of this paper was arranged by Editor M. Thumm.

C. Paoloni is with the Engineering Department, Lancaster University, Lancaster LA1 4YW, U.K. (e-mail: c.paoloni@lancaster.ac.uk).

M. Mineo is with e2v Technologies, Chelmsford CM1 2QU, U.K. (e-mail: mauro.mineo@e2v.com).

M. Henry and P. G. Huggard are with the Millimetre Wave Technology Group, Science and Technology Facilities Council Rutherford Appleton Laboratory, Didcot OX11 0QX, U.K. (e-mail: manju.henry@stfc.ac.uk; peter.huggard@stfc.ac.uk).

Color versions of one or more of the figures in this paper are available online at http://ieeexplore.ieee.org.

Digital Object Identifier 10.1109/TED.2015.2480535

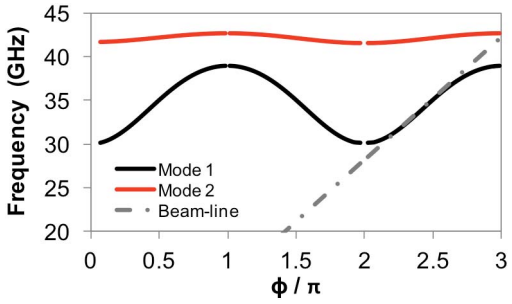

Fig. 2. Dispersion curves with the beam line superimposed. The dimensions of the DCW are shown in Fig. 1 and the beam voltage is 12 kV.

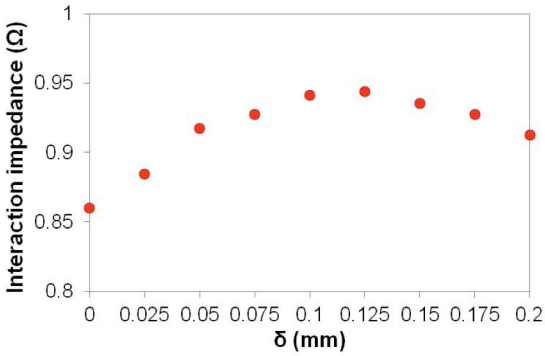

Fig. 3. Calculated interaction impedance as a function of the height of the on-axis electron beam above the tops of the pillars for 34 GHz and 12-kV beam voltage.

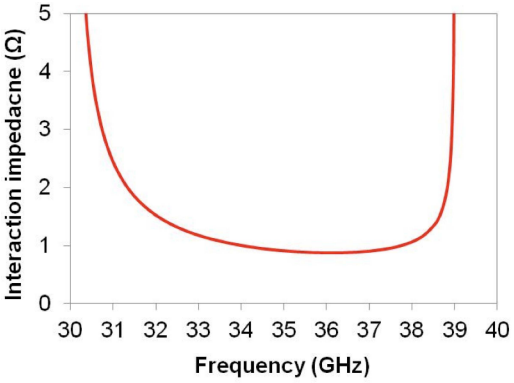

Fig. 4. Calculated interaction impedance as a function of frequency for an on-axis beam at height $\delta = 0.12$ mm above the pillar tops.

field interaction zone is concentrated in the central region of the SWS, between the rows of pillars. This concentration of field away from the walls reduces the criticality of the lid to the channel connection.

The wideband properties of the DCW in forward wave mode as an SWS for a 0.22-THz TWT have yielded a bandwidth wider than 12% [10]. The scalable nature of the DCW makes it suitable for use in the microwave to submillimeter wave range. The DCWs have already been fabricated for higher frequencies by the scale appropriate microfabrication processes: by deep X-ray LIGA [11] at 1 THz and by high resolution computer numerical control (CNC) milling [12] at 0.346 THz. We now describe the novel design, the application of the conventional precision CNC machining and the test of a Ka-band (32–37 GHz) DCW TWT.

II. Double Corrugated Waveguide Design

A DCW was designed as an SWS for a TWT operating in the 32–37 GHz frequency band, representing about 15% fractional bandwidth. The beam voltage was selected at 12 kV to minimize the power supply size. In contrast to the helical SWS that operates in the fundamental space harmonic, the DCW has to operate in the first space harmonic to support a relatively low electron accelerating potential and to provide wideband interaction [11]. The first space harmonic provides a lower interaction impedance than the fundamental, but still delivers sufficient interaction impedance to assure a significant energy transfer from the electron beam to the millimeter wave field, with consequently adequate TWT gain.

The operating frequency band is derived from the dispersion curves, considering the region between lower and upper cutoff frequencies. The dispersion curves of the two first modes were computed by CST MWS [13] (Fig. 2). The large gap between the fundamental mode and the second mode means that the latter plays no part in the interaction. The useful portion of the dispersion curve, which overlaps with the beam line for the selected beam voltage, is the phase shift region in the 2π–3π range. A useful frequency band from 31–37 GHz, corresponding to ∼17% percentage bandwidth, was obtained for the optimized structure with ∼12-kV beam voltage. The few millimeter dimensions of this structure, given in Fig. 1, make it suitable for direct manufacture with a precision CNC mill.

A study was undertaken to find the position of the electron beam that maximizes the interaction impedance. Beam energy (12 kV) and frequency (34 GHz) were held constant for this modeling. As the electron beam propagates in the symmetry plane, this paper reduces to finding the best vertical position, δ, between the beam axis and the top of the pillars. The results plotted in Fig. 3 show a plateau for 0.10 mm $\leq \delta \leq$ 0.14 mm.

An optimum value of $\delta = 0.12$ mm is, therefore, used to calculate the frequency response of the interaction impedance. Fig. 4 shows that this has a weak frequency dependence, and is ≈1 Ohm from 32 to 37 GHz.

The SWS for a TWT requires low loss and low reflectivity input and output couplers to standard rectangular waveguide over the entire operating bandwidth. Efficient wideband coupling is obtained by properly tapering the height of the pillars and the heights and width of the waveguide enclosure. Two coupling approaches have been investigated. One, based on linear tapering of the pillars along the beam channel, i.e., in the longitudinal direction of the TWT, is easier to fabricate, but requires a longer structure with the consequent need for a larger volume magnetic field. The second, novel, approach is based on bending the DCW through 90°. This permits the positioning of tapered coupling sections orthogonally to the interaction section. The manufacture and S-parameter characterization of these two approaches to the DCW TWT are described below.

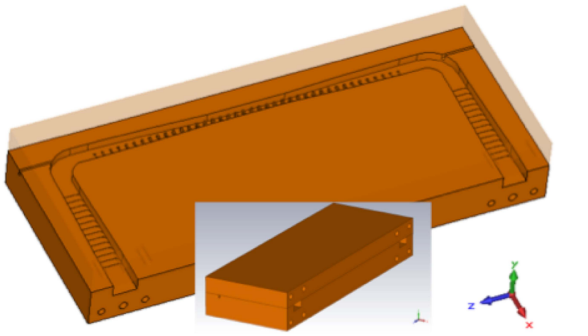

Fig. 5. Pillar layout and channel tapering in the linear coupler DCW TWT. Inset: assembled structure with its WR-28 waveguide flanges and hole for electron beam injection/extraction.

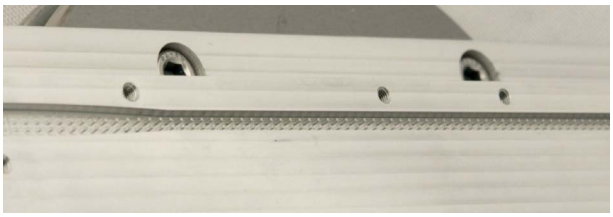

Fig. 6. Photograph of a part of the interaction region of the aluminum DCW before attachment of the lid.

III. Linear Coupler DCW SWS

The linear coupler DCW SWS topology consists of an uniform interaction section with both ends terminated with sections where the pillar height is linearly tapering to zero (Fig. 5). This enables wideband coupling between the TE_{10} mode of rectangular waveguide and the hybrid mode supported by the DCW.

The optimized DCW comprises a 40 period interaction region and two linear DCW transitions connected by a bent waveguide to the WR-28 flanges. Each DCW transition includes 15 pillar rows linear tapered in height. The waveguide enclosure has a sinusoidal tapered profile toward the bend to improve the matching. The structure is fabricated in two parts. One is the DCW with the couplers as shown in Fig. 5, and the other is a plane metal lid. Hex-head machine screws are used to fix the two parts together.

Aluminum was chosen as metal for the first prototype for its easier machining in comparison with copper. The structure was machined on a KERN Pyramid milling machine. A photograph of part of the interaction region is shown in Fig. 6.

The S-parameters of the realized DCW were measured and compared with the 3-D electromagnetic simulations. Good agreement, Fig. 7, is obtained for S_{11} and S_{21}. In particular, the maximum frequency difference is of about 1%. The conductivity of aluminum was reduced in the calculations to $\sigma_{Al} = 1.72 \times 10^7$ S/m to account for the losses due to oxidation. This is the first cold test validation of a Ka-band DCW which has been manufactured by CNC milling. Good agreement with predictions also demonstrates the simulator accuracy in modeling the DCW.

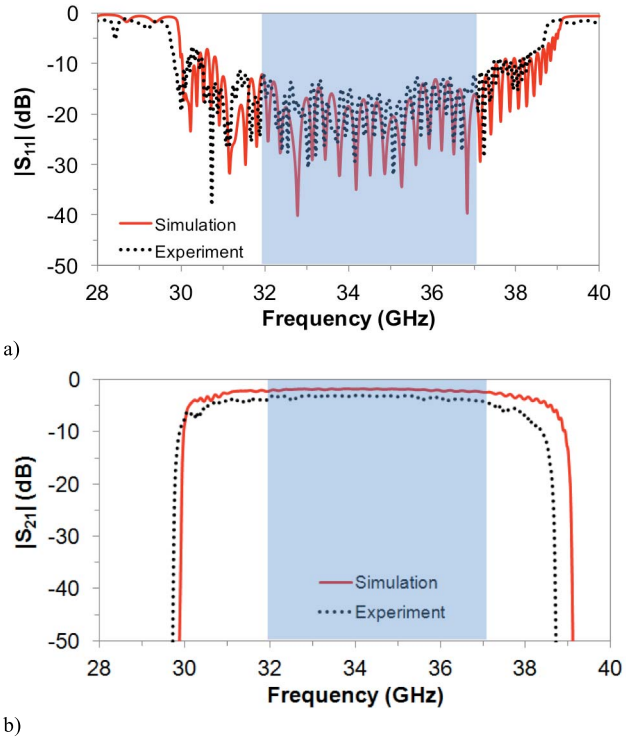

Fig. 7. Comparison between measurements, red, and simulations, black, of (a) S_{11} and (b) S_{21} for the linear coupler DCW.

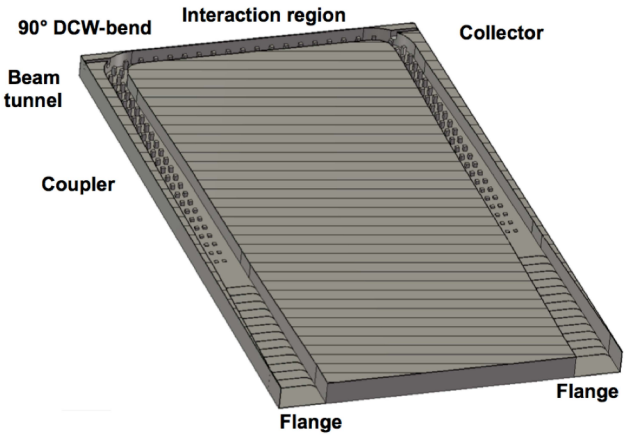

Fig. 8. DCW SWS with bends, sections with tapered pillar heights, and step-tapered waveguide to connect to WR-28 flanges.

IV. DCW With Bends for Lateral Coupling

The linear coupler DCW SWS includes two regions, in the range of 24% of overall length, where the electron beam is partially modulated and only a very weak interaction is present. However, the electron beam traveling in these regions still needs magnetic focusing. In other words, the regions increase the volume without adding to the gain. A novel approach, based on a 90° bending of the DCW at the ends of the main interaction region, has been developed. This places the regions of weak interaction, with tapered pillars, orthogonal to the main gain section (Fig. 8). This approach permits a substantial reduction of the overall TWT length.

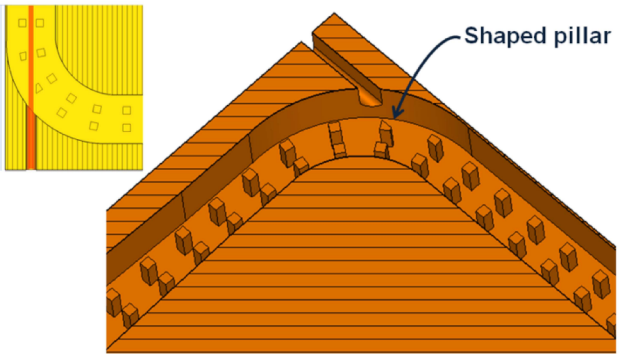

Fig. 9. Details of the beam aperture region of the bent DCW with optimized pillar locations and one pillar modified to avoid intersecting the electron beam. Inset: example of the beam hitting a pillar in the unmodified DCW.

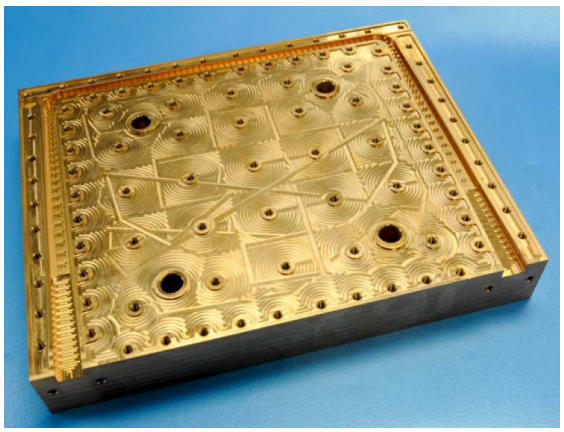

Fig. 10. DCW SWS with bent couplers realized in copper alloy. The TWT with the 50 period interaction region is shown.

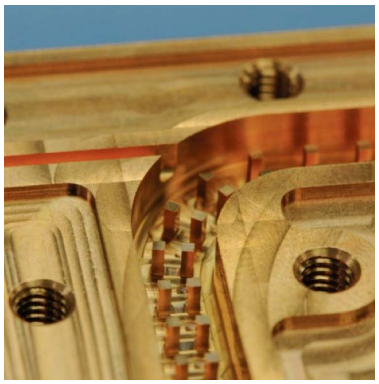

Fig. 11. Detail of the bent DCW section: the electron beam channel and modified pillar are also visible.

A. Design

Fig. 8 shows the complete optimized millimeter wave structure. The DCW is bent at 90° with respect to the beam tunnel and the collector end. After each bend follows a DCW to rectangular waveguide transition, to couple the hybrid mode to the TE_{10} mode. Twenty pairs of DCW pillars are tapered in height and in period length in the DCW transition. The DCW enclosure width has a sinusoidal profile. The total length of the DCW transition is 69 mm. Finally, a matching section connect the DCW transition to the WR-28 flange.

Bending the DCW near the electron beam tunnels requires that pillars be locally modified to prevent them intersecting the beam. An optimization of the position and shape of the pillars in the bend regions was performed to maintain simultaneously the electrical behavior of the DCW, satisfy the fabrication constrains, and permit the electron beam to pass.

It was found that by positioning the pillars correctly, only one pillar needed modification to maintain the electron beam flow. A portion of this pillar on the line of the beam was cut away (Fig. 9), so that it had an approximately triangular cross section. Numerical simulations confirmed that that this modified pillar geometry did not affect the electromagnetic behavior.

B. Fabrication and Measurements

Two DCWs with bent sections were fabricated in tellurium-copper alloy. The two structures differed only in the number of periods in the interaction region: one had 30 and the second 50 periods. Having SWSs with different lengths available permits experimental evaluation of the dispersion curve. Fig. 10 shows a photograph of the 50 period DCW before the lid was attached. The quality of the mechanical fabrication is shown in Fig. 11, where the detail of the DCW bend is shown.

A comparison of the measurements and CST MWS simulation (reduced copper conductivity $\sigma_{Cu} = 3.9 \times 10^7$ S/m) of the 50 period DCW in the Ka-band is shown in Fig. 12. There is excellent agreement. Measured $|S_{11}|$ is better than -20 dB and transmission losses are <2 dB over the 32–37-GHz frequency band.

The experimental dispersion curve of the DCW is computed by the difference in the measured phases of the transmitted signal between the 30 and 50 period structures. The following equation describes this phase difference:

$$\Delta\varphi(f)/\Delta L = \beta(f) \cdot p \tag{1}$$

where $\Delta\varphi(f)$ is the phase difference as a function of frequency f, ΔL is the DCW length difference, $\beta(f)$ is the propagation constant, and p is the period of the DCW.

A frequency difference lower than 1% is obtained between the measurements and the simulation (Fig. 13). The simulations were performed using both the eigenmode solver and the frequency domain solver. The agreement also demonstrates the high quality of the fabrication process by the CNC milling and the accuracy of the 3-D electromagnetic simulator. The loss of the copper structure, $\approx$2 dB in the operating band, is also in good agreement with the simulations. This is in contrast with the excess loss of the aluminum DCW, Fig. 6, which may arise from poor connection at the channel/lid interface due to surface oxidization.

C. DCW TWT Design and Simulations

The performance of a millimeter wave TWT using the DCW with bent sections as SWS has been analyzed. The DCW unit dimensions are the same reported in Section II (Fig. 1). A beam voltage of 12 kV, a beam current of 200 mA,

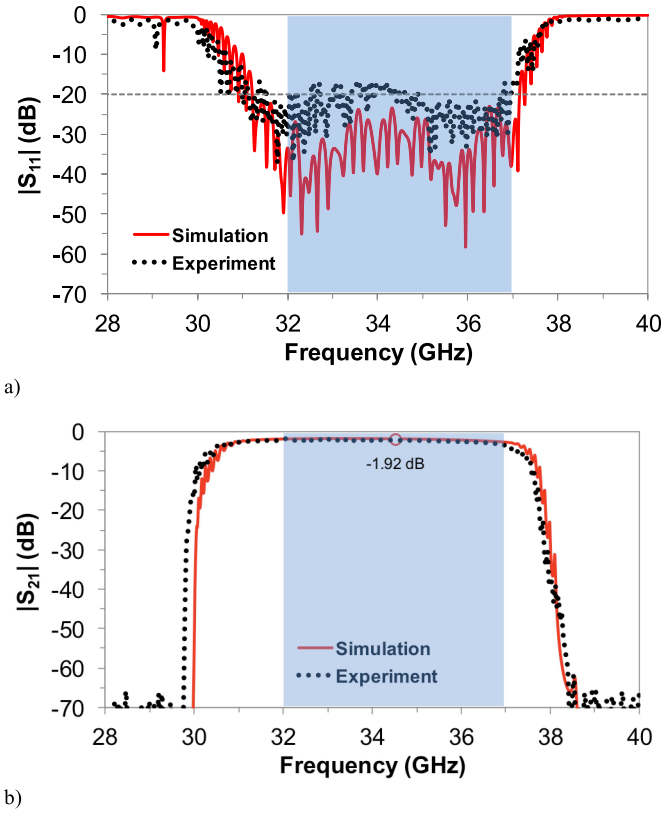

Fig. 12. Comparison of measured and simulated S-parameters for the 50 period DCW. (a) S_{11}. (b) S_{21}. Solid (broken) lines—predictions (measurements). Insertion loss is marginally < 2 dB in the center of the operating band.

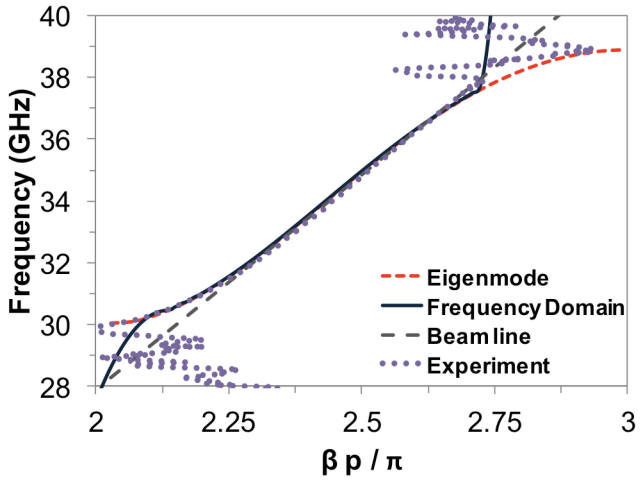

Fig. 13. Comparison of the measured and simulated dispersion curve for the DCW with bends. CST-E and CST-FD refer to CST eigenmode and frequency domain predictions, respectively, while experimental data are shown by the lilac dotted line.

and 250-μm beam radius are assumed. A uniform magnetic field of 0.3 T is applied. The input power is 100 mW.

To evaluate the millimeter wave gain, a DCW TWT with 80 periods in the interaction region was simulated by CST-Particle Studio. A relatively flat gain of about 25 dB, [Fig. 14(a)] and an output power in the 18 to 29 W range were

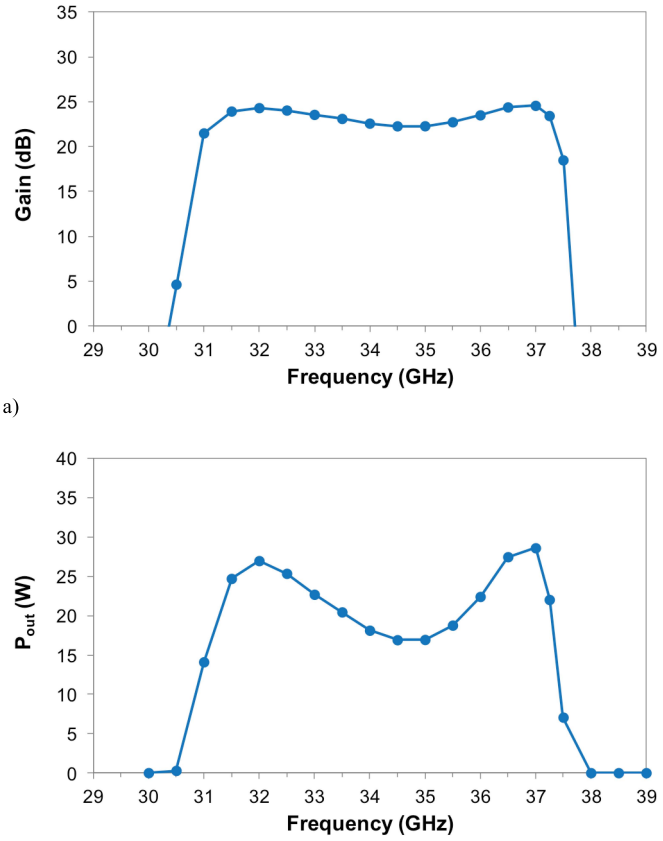

Fig. 14. (a) and (b) Predicted TWT gain (dB) and output power (W) as a function of frequency for a 80 period TWT. TWT dimensions are given in Fig. 1, beam current is 200 mA at 12 kV, and input power is 100 mW.

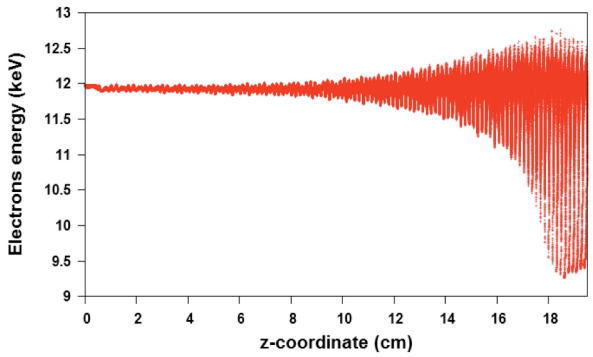

Fig. 15. Electron energy along the DCW TWT.

demonstrated in the 32–37-GHz frequency range [Fig. 14(b)]. The low and high frequency peaks are thought to arise from the relatively wideband, as the interaction condition changes for the different frequencies. At low frequency the interaction impedance is high, while at the high frequency the synchronism is better. The electron energy shown in Fig. 15 demonstrates the high level of interaction. The high gain and output power demonstrates the promise of the DCW. Improved performance could be obtained by using a multisection TWTs.

V. Conclusion

The DCW has been demonstrated to be effective SWS, which overcomes the difficult fabrication and high cost of helical SWS at millimeter wave frequencies. A novel solution to realize a compact TWT with improved performance by bending the DCW is presented. S-parameter measurements on DCW TWTs demonstrate low loss, wide 31–37-GHz bandwidth and excellent agreement with simulations. Predictions show up gains to 25 dB and output power up to 25 W for 12-kV beams at 200 mA and a 0.3 T axial magnetic field. This promising performance demonstrates the potential importance of the DCW in the field of vacuum electron devices as a solution for a new family of affordable millimeter wave TWTs.

Acknowledgment

The authors would like to thank A. Wood, M. Duffield, D. Bowler, and P. John of e2v for their continued support and advice in the course of this project, M. Beardsley and L. Bushnell of STFC RAL Space for their precise fabrication of the DCW structures, and K. Parow-Souchon for the accurate measurements.

References

[1] C. K. Chong and W. L. Menninger, "Latest advancements in high-power millimeter-wave helix TWTs," *IEEE Trans. Plasma Sci.*, vol. 38, no. 6, pp. 1227–1238, Jun. 2010.

[2] C. K. Chong *et al.*, "High power millimeter wave helix TWT programs at L-3 ETI," in *Proc. IEEE 14th Int. Vac. Electron. Conf. (IVEC)*, May 2013, pp. 1–2.

[3] R. H. Abrams, B. Levush, A. A. Mondelli, and R. K. Parker, "Vacuum electronics for the 21st century," *IEEE Microw. Mag.*, vol. 2, no. 3, pp. 61–72, Sep. 2001.

[4] W. L. Menninger, N. R. Robbins, D. R. Dibb, and D. E. Lewis, "Power flexible Ka-band traveling wave tube amplifiers of up to 250-W RF for space communications," *IEEE Trans. Electron Devices*, vol. 54, no. 2, pp. 181–187, Feb. 2007.

[5] C. K. Chong *et al.*, "Development of high-power Ka-band and Q-band helix-TWTs," *IEEE Trans. Electron Devices*, vol. 52, no. 5, pp. 653–659, May 2005.

[6] S. Sengele, M. L. Barsanti, T. A. Hargreavesm, C. M. Armstrong, J. H. Booske, and Y. Y. Lau, "Impact of random fabrication errors on fundamental forward-wave small-signal gain and bandwidth in traveling-wave tubes with finite-space-charge electron beams," *IEEE Trans. Electron Devices*, vol. 60, no. 3, pp. 1221–1227, Mar. 2013.

[7] H. Gong, Y. Gong, T. Tang, J. Xu, and W.-X. Wang, "Experimental investigation of a high-power Ka-band folded waveguide traveling-wave tube," *IEEE Trans. Electron Devices*, vol. 58, no. 7, pp. 2159–2163, Jul. 2011.

[8] A. J. Theiss, C. J. Meadows, R. Freeman, R. B. True, J. M. Martin, and K. L. Montgomery, "High-average-power W-band TWT development," *IEEE Trans. Plasma Sci.*, vol. 38, no. 6, pp. 1239–1243, Jun. 2010.

[9] M. Mineo and C. Paoloni, "Double-corrugated rectangular waveguide slow-wave structure for terahertz vacuum devices," *IEEE Trans. Electron Devices*, vol. 57, no. 11, pp. 3169–3175, Nov. 2010.

[10] C. Paoloni and M. Mineo, "Double corrugated waveguide for G-band traveling wave tubes," *IEEE Trans. Electron Devices*, vol. 61, no. 12, pp. 4259–4263, Dec. 2014.

[11] C. Paoloni *et al.*, "Design and realization aspects of 1-THz cascade backward wave amplifier based on double corrugated waveguide," *IEEE Trans. Electron Devices*, vol. 60, no. 3, pp. 1236–1243, Mar. 2013.

[12] C. Paoloni *et al.*, "THz backward-wave oscillators for plasma diagnostic in nuclear fusion," in *Proc. IEEE Int. Conf. Plasma Sci.*, Antalya, Turkey, May 2015, p. 1.

[13] CST AG, Darmstadt, Germany. *CST STUDIO SUITE*. [Online]. Available: http://www.cst.com

Claudio Paoloni (M'86–SM'11) received the Laurea degree in electronic engineering from the University of Rome "Sapienza", Italy, in 1984.

He joined as Researcher the Electronic Engineering Department, University of Roma "Tor Vergata", Italy. Since 2012, he has been a Professor of Electronics with the Engineering Department, Lancaster University, U.K. He is Coordinator of the Horizon2020 TWEETHER project. He is member of the IEEE EDS Vacuum Electronics Technical Committee. He is the Head of the Engineering Department.

Mauro Mineo received the Ph.D. degree in telecommunication and microelectronic engineering from the University of Rome Tor Vergata, Rome, Italy.

He was a Research Associate with the Engineering Department, Lancaster University, Lancaster, U.K., from 2012 to 2015. Since 2015, he has been with e2v Technologies Ltd., Chelmsford, U.K., as an RF/Microwave Modelling Engineer.

Manju Henry received the master's and Ph.D. degrees in electronic engineering from Cochin University, Kochi, India.

She joined the Millimetre Wave Technology Group, STFC Rutherford Appleton Laboratory, Didcot, U.K., in 2007. She has held technical and management roles in EU and ESA programs.

Dr. Henry undertakes passive mm-wave system design for atmospheric sounding and astronomy, active system development for meteorology, and security imaging.

Peter G. Huggard (SM'12) received the B.A. degree in experimental physics and the Ph.D. degree from the University of Dublin, Trinity College Dublin, Dublin, Ireland, in 1986 and 1991, respectively.

He has been a member of the Millimetre Wave Technology Group with the STFC Rutherford Appleton Laboratory, Didcot, U.K., since 2000. His current research interests include developing sources and detectors for gigahertz and terahertz radiation.